Open Access
Stechnolock: Chemical Engineering Science

RESEARCH ARTICLE

Adaptive and Tunable Flexible Composite Fibers for Integrated Infrared/Visual Stealth

Qingyi Ma[2], Lifei Chen[1,*], Yanjie Chen[1], Li Zhang[2], Xin Wang[1], Jiaojiao Xing, Xueling Zhao[1], Jifen Wang[2], Huaqing Xie[1]

[1]*School of Energy and Material Engineering, Shanghai Polytechnic University, Shanghai 201209, P. R. China*
[2]*School of Resources and Environmental Engineering, Shanghai Polytechnic University, Shanghai 201209, P. R. China*

[*]**Corresponding Author:** Lifei Chen, School of Energy and Material Engineering, Shanghai Polytechnic University, Shanghai 201209, P. R. China, Tel.: 13611845882, E-mail: lfchen@sspu.edu.cn

Citation: Qingyi Ma, Lifei Chen, Yanjie Chen, Li Zhang, Xin Wang (2024) Adaptive and Tunable Flexible Composite Fibers for Integrated Infrared/Visual Stealth, SMP Chem Eng Sci, 2: 1-14

Abstract

Currently, single-function stealth technology for visual or infrared stealth has made great progress, but it is difficult to adjust to the various needs of complex situations. Thus, there are still challenges in avoiding visible and infrared light at the same time for monitoring. Based on that, this experiment uses wet spinning technology to produce a flexible composite fiber which is both infrared and visual stealthy. The fibers have adjustable phase transition temperatures (from 15°C to 38°C), excellent thermal energy storage capacity (enthalpy up to 147.09 J/g), outstanding cycling stability (100 cycles) and great mechanical properties. Furthermore, the fiber's adaptive color-changing effect can well achieve the stealth effect in the visual environment, and match the various scenarios from the ocean to the jungle to the desert in the visible light range. Combined with excellent thermal management and thermoregulation, the fiber enables simultaneous day and night infrared stealth, which overcomes the shortcomings of traditional stealth technologies. This advanced infrared/visual stealth technology will offer a wide range of applications in human stealth, equipment stealth, military target stealth, and other fields.

Keywords: Phase change thermoregulation, Thermal management, Infrared/Visual stealth, Flexible composite fiber, Multifunctional properties

Introduction

The principle of 'survival of the fittest' is an unchanging law in the natural world. Just like chameleons, many species in the natural world employ visual camouflage as a clever strategy for self-protection. Inspired by these animals, visual stealth technology has emerged[1-3]. So far, visually stealth technology has been regarded as a necessary means of concealment, employing transmission or reflection to match the background colors within the visible light spectrum[4, 5]. By utilizing visual stealth, equipment or individuals can seamlessly blend into their environment, achieving effective reconnaissance and anti-reconnaissance effects[6, 7]. Ma et al. have developed a light-driven adaptive visual stealth system that utilizes folding to switch between stealth and exposure states[8]. However, the visual stealth technology achieved through structural adjustments is complex to operate and has certain limitations[9]. Therefore, current research typically utilizes surface coatings and stimulus-responsive color-changing methods to achieve visual stealth effects. Coating composite materials are a simple and commonly used strategy, but their fixed color is not suitable for tactical camouflage in changing environments[10, 11]. Stimulus-responsive color-changing methods manipulate the light-matter interaction to achieve dynamic color changes, such as thermochromic, mechanochromic, photochromic, and electrochromic methods[12]. Among these methods, thermochromic materials activated by light-heat have efficient and convenient characteristics, making them particularly suitable for adaptive outdoor camouflage[13]. For example, Li et al. combined the bottom of anisotropic MXene/Reduced Graphene oxide hybrid aerogel with paraffin phase change material (PCM), and added a thermochromic coating layer on its surface to prepare a three-layer composite material for simultaneous visible light and infrared dual camouflage[14].

Up to present, numerous reports have highlighted various adaptive stealth materials and visual concealment systems. However, with the continuous progress and development of technology, advanced infrared detection techniques can identify objects through temperature monitoring and the differentiation of infrared variances[15]. Under the surveillance of infrared cameras, no object with a temperature above 0 K can evade detection. Even accomplished practitioners of visual stealth find it challenging to escape scrutiny. Consequently, relying solely on visual concealment proves insufficient for achieving comprehensive camouflage[16, 17]. In order to prevent the detection of targets, the integration of visual and infrared concealment is imperative. Common methods employed for achieving infrared concealment include adjusting infrared emissivity and controlling surface temperature[18, 19]. Various low-emissivity materials, such as MXene films and metal coatings, have been developed. However, in most cases, the approach of adjusting infrared emissivity can only temporarily conceal the target within a matching background, making it difficult to achieve widespread applications. In contrast, materials with temperature regulation properties can better satisfy the demands of infrared concealment under complex and variable conditions[20-22]. According to previous research, thermal management materials such as thermoelectric materials and phase-change materials are typically utilized to regulate the surface temperature of objects for temperature control purposes. The PCMs, serving as clean and renewable heat storage materials, represent a superb category of thermal management materials. They exhibit strong heat management capabilities, a diverse range of types, non-toxic characteristics and convenient usage[23-25]. Moreover, they maintain a certain temperature during phase transitions, and demonstrate excellent stability and environmentally friendly[26]. Consequently, they have got significant attention in the realm of infrared stealth research. For instance, Wen et al. have conceived and fabricated an ultra-thin MXene-based composite film, being applicable across a broad spectrum of fields including thermal infrared stealth, electromagnetic wave shielding, and energy conversion[27]. Zhou et al., by integrating a hydrogel substrate with phase change microspheres, have prepared a flexible phase change hydrogel with outstanding thermal physical properties, capable of achieving infrared stealth functionality in mid to low-temperature environments[28]. Despite extensive research, the design of composites to avoid synergistic visible/infrared detection in complex situations remains a difficulty. The synthesis of stealth materials possessing high flexibility and simultaneously rapid response characteristics remains a hard challenge[29, 30].

To solve the mentioned challenges, this study employs a wet spinning method to design and fabricate a composite fiber (BCFs) that integrates both infrared and visual stealth capabilities. The BCFs utilizes the thermochromic effect of color-changing microcapsules to achieve visual concealment in visible light environments. Simultaneously, the heat absorption and release properties of different PCMs are used to regulate the temperature difference between the protected object's surface and the surrounding environment, thereby realizing infrared stealth functionality. In summary, as temperature fluctuates, the BCFs autonomously adjusts the surface temperature of the target object to match the background temperature. Furthermore, the temperature-induced color changes enable the BCFs to adapt to the surrounding environment, achieving dual concealment effects in both infrared and visual domains. The prepared BCFs are expected to play an important role in applications in human stealth, equipment stealth, military target stealth and other fields.

Experimental

Materials

Thermoplastic polyurethane powder (PU, Mn ≈ 100,000), procured from Hefei Yuanli Instrument Technology Co., Ltd. (Hefei, China); thermochromic microcapsules (TMC), obtained from Guangzhou Shengse Technology Co., Ltd. (Guangzhou, China); N, N-dimethylformamide (DMF), n-hexadecane, n-octadecane, and n-eicosane, sourced from Titan Technology Co., Ltd. (Shanghai, China).

Preparation of spinning solution

Initially, various masses of thermochromic powder were measured and added to 20 ml of DMF, followed by ultrasonication for 10 minutes to ensure thorough mixing. Subsequently, different masses of PU were introduced into the mixed solution, and the mixture was stirred for 12 hours to prepare a uniformly blended spinning solution.

Preparation of thermochromic fibers with hollow structures

Utilizing the coaxial wet spinning method, hollow-structured thermochromic fibers were prepared with deionized water as the coagulation bath. Initially, deionized water and the PU/TMC/DMF spinning solution were separately drawn using a syringe pump. The coaxial spinning nozzle was installed so that deionized water and spinning solution were extruded from the inner/outer channels at rates of 13 ml/h and 15 ml/h, respectively, and the diameters of the inner and outer channels were 0.4 mm and 1.1 mm. After configuring the parameters, the spinning solution was extruded from the nozzle into the water bath, forming a core-shell structure. After solidification, the fibers were immersed in deionized water for 30 minutes and air-dried, resulting in thermochromic fibers with a hollow structure (PU-TMC). By varying the TMC content, a series of thermochromic fibers with different proportions were prepared and designated as PU-TMC_X, where X represents the ratio of the mass of TMC to the solvent content in the fiber. The fibers were named PU-$TMC_{0.05}$, PU-$TMC_{0.15}$, PU-$TMC_{0.25}$, and PU-$TMC_{0.35}$.

Preparation of flexible composite fibers integrating infrared /visual stealth

Using a syringe and an extended needle, molten n-hexadecane, n-octadecane, and n-eicosane were individually injected into the prepared hollow fibers. Injection commenced from one end of the fiber until liquid emerged from the other end. The fiber was continuously rotated to ensure thorough filling of the hollow interior with PCM. Subsequently, the fiber ends were sealed with spinning solution and solidified in the water bath. Depending on the injected PCM, the fibers were designated as PU-TMC_X@HD, PU-TMC_X@OD, and PU-TMC_X@EO. After the completion of composite fiber preparation, the excellent flexibility allowed manual weaving of the fibers into composite fiber films or textiles using a knitting needle. Fig.1a illustrates the entire manufacturing process of the flexible composite fiber (BCFs).

Characterization

The morphology of fibers was examined by Cold Field-Emission Scanning Electron Microscope (SEM, Japan Hitachi, Regulus 8100). Thermal analysis of each sample (~ 3.0 mg) was performed by using a differential scanning calorimeter (DSC) (American TA DSC 250) with a heating and cooling rate of 5°C min^{-1} from 0 to 60 °C. The thermal stability of the sample was tested by thermal gravimetric analysis (TGA) (American TA TGA Q5000) with a heating rate of 20°C min^{-1} from 30 to 700°C under nitrogen flow. The mechanical properties of the samples were tested by universal testing machine (China Dongri Instrument) with a tensile speed of 10 mm min^{-1}.

Results and Discussion

Preparation and Structural Analysis of BCFs

During the spinning process, a coaxial wet spinning process based on the non-solvent-induced phase separation principle was employed to design the BCFs with a hollow structure. The formation mechanism of the BCFs is illustrated in Fig.1b. When the spinning solution is injected into the coagulation bath, the solvent (DMF) in the spinning solution can easily exchange with water (the non-solvent in the coagulation bath) due to the hydrophilic amino acid ester bonds in the PU polymer. In the water bath, dispersed PU chains and TMC molecules encounter the non-solvent, leading to rapid diffusion between water and DMF solvents. This results in the aggregation of TMC and PU chains, and the TMC/PU layer solidifies in the water. After phase separation and drying, the BCFs with a hollow structure is obtained.

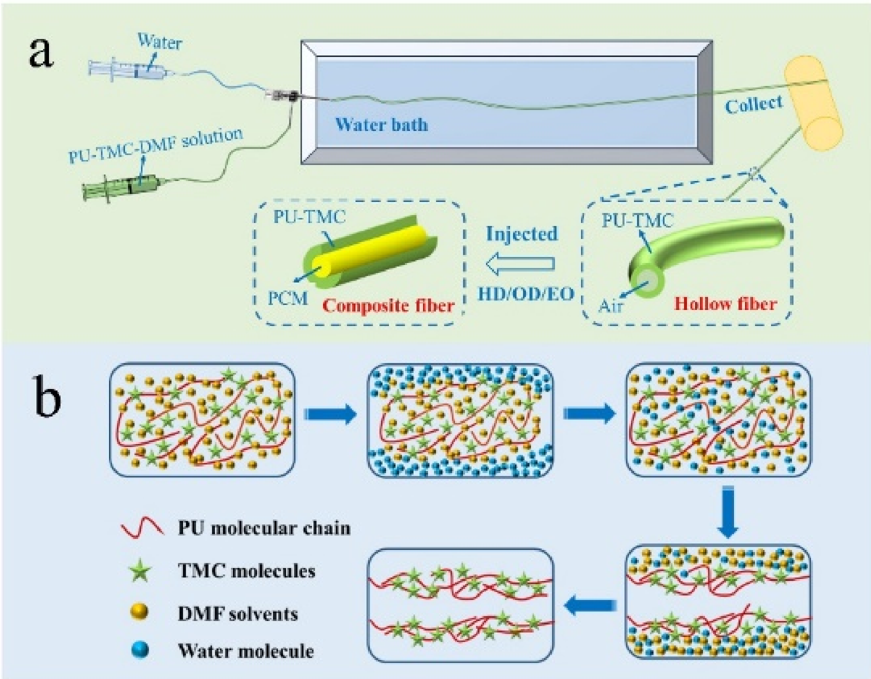

Figure 1: (a) Schematic diagram of the preparation process of BCFs. (b) Schematic of the preparation mechanism of BCFs

The structure of the composite fiber produced by the wet spinning process is determined by phase transformation process parameters such as the viscosity of the spinning solution, flow rate, solubility (solvent/non-solvent interaction), and solidification rate. Therefore, spinning solutions with different concentrations (PU contents of 30%, 40%, 50%, 55%, 60%) were prepared to evaluate the fiber-forming conditions and determine the optimal ratio. Experimental results revealed that at a PU content of 30% (Fig.2a), the solution was difficult to shape in the water bath due to insufficient viscosity. With an increase in PU content to 40%(Fig.2b), the fiber-forming effect was still poor because of the higher solvent content, making rapid exchange challenging. When the PU content in the solution reached 50%, 55% and 60%, well-formed fiber samples were prepared. The optimal experimental ratio was selected through microscopic morphology comparisons. SEM images with a concentration of 55% BCF showed a clear and perfect hollow structure (Fig.2c). The thickness of the fiber shell was ~ 120 μm, and the diameter of the hollow was ~ 1.19 mm (Fig.2d). The PU layer on the fiber surface exhibited dense accumulation, with the 55% PU content demonstrating the smoothest surface structure. Considering all aspects, the PU content of 55% was selected as the optimal concentration for the support material.

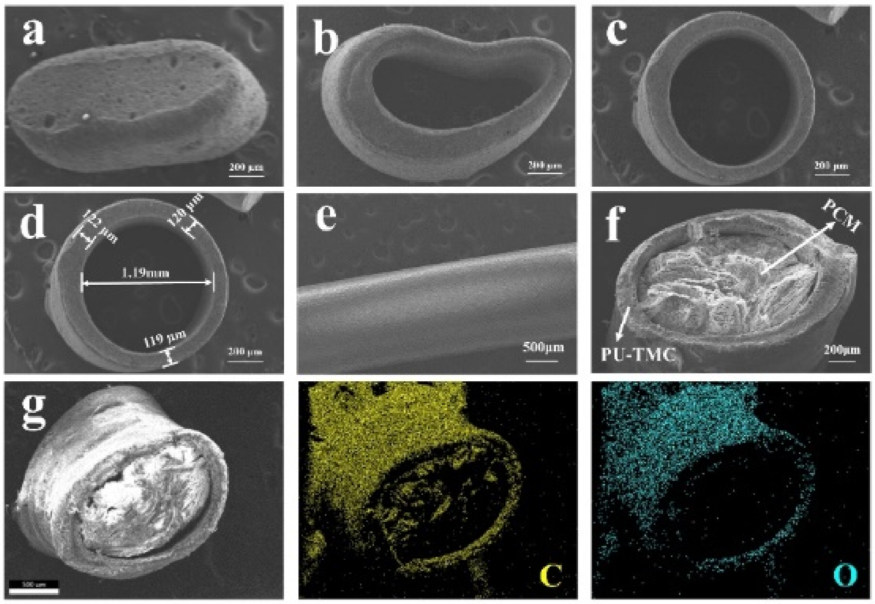

Figure 2: (a) SEM of PU-TMC samples with different PU contents: (a) 30%, (b) 40%, (c) 55%; (d) Fiber pore size and (e) fiber surface with 55% PU content; (f) Cross-section of the sample; (g) EDS of the sample after injection of PCM

SEM images of the BCFs after the addition of TMC and injection of n-octadecane (OD) are depicted in Fig.2e, f. It can be observed that the fiber surface remains smooth, indicating that the addition of TMC has no discernible impact on the fiber-forming effect. The microscopic morphology of the cross-section reveals that a significant amount of OD is enveloped by the TMC/PU sheath, demonstrating that effective coating of OD can be achieved through the injection method. Energy-dispersive X-ray spectroscopy (EDS) images further confirm the dense encapsulation of OD by the TMC/PU layer (Fig.2g).

Thermoregulation and Thermal Stability of BCFs

As is well known, the thermal regulation performance is a fundamental characteristic of temperature-regulating energy storage materials, and the heat absorption/release capacity of BCFs plays a crucial role in their practical applications. The hollow structure of the fibers endows BCFs a significant encapsulation capacity for PCMs. Consequently, BCFs exhibit a high enthalpy, a key attribute for assessing thermal energy storage capacity. The phase change temperatures and heat storage capacities of fiber samples injected with different PCMs were measured using differential scanning calorimetry (DSC), and the obtained DSC curves are presented in Fig.3 a-c. The phase change temperature and latent heat values for different samples are listed in Table 1, where the latent heat includes both crystallization enthalpy (ΔH_c) and melting enthalpy (ΔH_m), two crucial parameters representing the thermal energy storage capacity of PCMs.

From the DSC curves, it is evident that the DSC curves of all BCFs are similar to those of pure PCMs. These curves effectively show that PCM exhibits regular phase transition behavior within the BCFs. From the Table 1, it is clear that depending on the injected PCM, the fibers possess a broad range of phase transition temperatures within the range of 15°C to 38°C. The maximum latent heat capacity for pure eicosane material reaches up to 206.4 J/g. The fibers injected with different PCMs exhibit a decrease in phase transition enthalpy compared to pure PCM materials. Nevertheless, the PU-$TMC_{0.25}$@EO fiber still exhibits a phase transition enthalpy value of 114 J/g, significantly higher than values reported in other literature.

Table 1: Thermal performance parameters of BCF

Sample	Types of PCM injected	T_m (°C)	ΔH_m ($J \cdot g^{-1}$)	T_c (°C)	ΔH_c ($J \cdot g^{-1}$)	E_{en} (%)	E_{es} (%)
Hexadecane	HD	20.1	164.9	15.5	168.4		
Octadecane	OD	29.8	192.2	24.7	200.5		
Eicosane	EO	38.5	198.0	33.3	206.4		
PU-TMC$_{0.25}$@HD	HD	20.5	147.1	15.0	144.6	89.2	87.5
PU-TMC$_{0.25}$@OD	OD	29.3	126.4	24.3	124.2	65.8	63.8
PU-TMC$_{0.25}$@EO	EO	37.9	114.0	30.5	110.3	57.6	56.9

Encapsulation rate and thermal storage efficiency are key characteristic parameters reflecting the thermal energy storage capacity of BCFs. The former characterizes the effective content of PCM within BCFs, while the latter describes the heat storage capacity of composite BCFs in reversible phase change processes. From Table 1, it can be observed that the hollow structure provides favorable encapsulation conditions for BCFs, resulting in samples with high encapsulation rates and thermal storage efficiency. Particularly, the actual encapsulation efficiency of the PU-TMC$_{0.25}$@HD sample reaches as high as 87.5%, indicating that the densely stacked PU/TMC shell effectively encapsulates the PCM. This is highly beneficial for effective thermal management of objects in different environments.

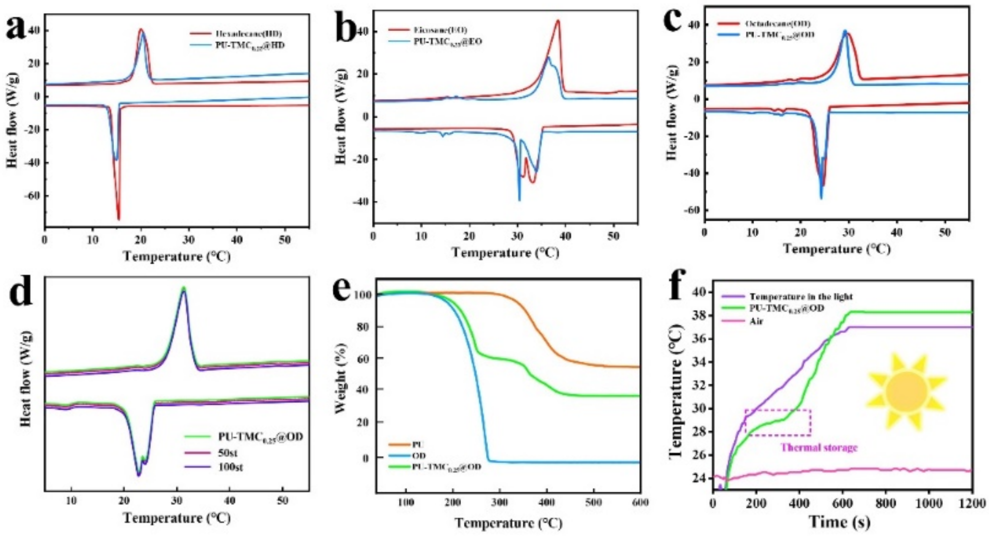

Figure 3: DSC curves for PCM and composite fiber samples: (a) HD and PU-TMC$_{0.25}$@HD (b) OD and PU-TMC$_{0.25}$@OD (c) EO and PU-TMC$_{0.25}$@EO; (c) TG curves of the sample (f) Temperature profile of PU-TMC$_{0.25}$@OD under sunlight

Thermal stability and reliability are crucial factors for practical applications. To assess this, temperature-controlled heating and cooling cycle tests were conducted, taking the PU-TMC$_{0.25}$@OD fiber sample as an example. The DSC results (Fig.3d) show that even after 100 cycles, the sample still exhibits a high degree of uniformity. The thermal regulation and storage capacity of the sample are almost unchanged compared to un-cycles, demonstrating exceptional thermal stability and reliability. This is highly advantageous for thermal energy storage and management. Thermal gravimetric analysis (TGA) curves display two thermal degradation stages for the BCFs sample (Fig.3e). The first decomposition stage occurring between 170–280°C corresponds to the decomposition of OD, while the second decomposition stage between 280–430°C is attributed to the decomposition of PU. Importantly, there is no significant weight loss observed below 100°C, indicating excellent thermal stability of the BCFs above the phase transition temperature, which is crucial for practical applications.

Under room temperature conditions, the temperature changes of the PU-TMC$_{0.25}$@OD fiber sample under sunlight (100 mW cm^{-2}) were monitored in real-time using a temperature recorder. Comparing the temperature curves (Fig.3f), it is evident that the temperature curve of the PU-$TMC_{0.25}$@OD fiber sample shows a distinct phase change plateau, while the pure PU fiber exhibits a gradual temperature increase after exposure to light without a phase change plateau. This indicates that OD within the composite fiber undergoes regular phase change behavior, and the high phase-change enthalpy of OD provides the composite fiber with higher energy storage capacity, enabling effective thermal energy storage. The test results further validate the practical applicability of the prepared samples, indicating that the prepared BCFs exhibits excellent temperature regulation and remarkable thermal energy storage capacity.

Mechanical Properties of BCFs

The tensile strength and breaking elongation of the fiber are crucial indicators characterizing the flexibility and elasticity of the fiber, determining the processing conditions of the fiber and the performance of the final products. Therefore, the mechanical properties of the fiber are of paramount importance for its practical applications. Through a universal testing machine, various mechanical parameters of the prepared BCFs were obtained, and the results are shown in Table 2. Fig.4 b-e shows the mechanical properties of the fibers. However, with an increase in TMC content, the maximum tension and tensile strength of the fiber significantly increase. This is because the substantial addition of TMC leads to a tighter molecular packing within the fiber, allowing the composite fiber to achieve greater tension and higher tensile strength.

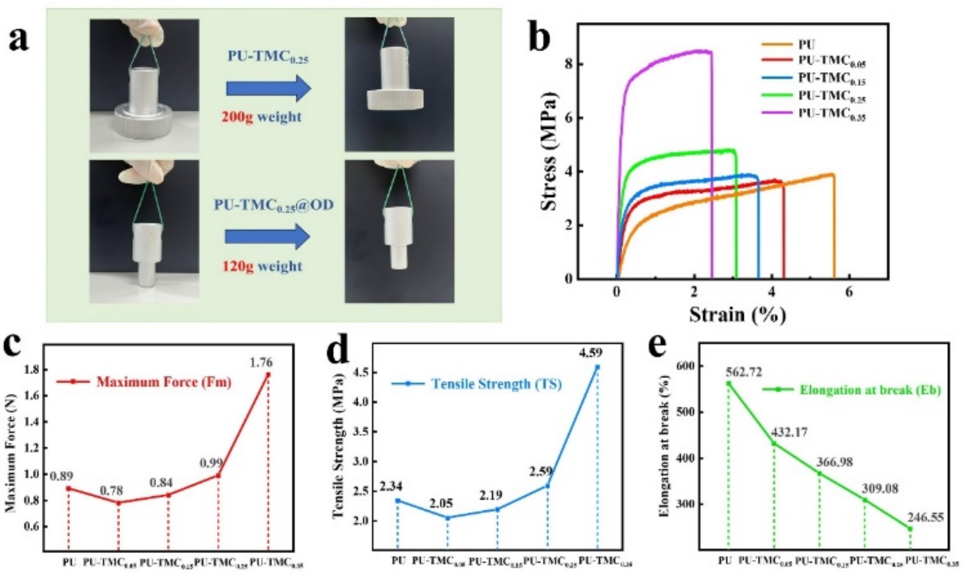

Figure 4: (a) Stretching of PU-$TMC_{0.25}$ and PU-$TMC_{0.25}$@OD under heavy loads; Mechanical curves of composite fibers with different TMC contents: (b) Stress-strain (c) maximum tensile force (d) tensile strength (e) elongation at break

In addition to tensile strength, the breaking elongation of the fiber is also crucial. Fibers with a high breaking elongation feel softer, but the breaking elongation should not be too high, as excessive elongation can lead to deformation. From the data, it can be observed that the breaking elongation of pure PU fiber is as high as 562.72%. With an increase in TMC content, the breaking elongation of the fiber shows a decreasing trend. This is because the high elasticity of the fiber comes from the contribution of PU molecular chains to strength. The effective arrangement of PU molecular chains along the spinning direction imparts extraordinary tensile and cyclic properties to pure PU fiber. The addition of TMC disrupts the interaction of PU polymer chains, thereby weakening the breaking elongation of the composite fiber. Nevertheless, even with a TMC content of 35%, the composite fiber still exhibits an impressive breaking elongation of 246.55%, demonstrating excellent mechanical performance. Additionally, in a heavy load test, PU-$TMC_{0.25}$ (only 10 cm long) can easily bear a weight load of 200 grams (Fig.4a). Even after injection with OD, the composite fiber can withstand a weight load of 120 grams without breaking (Fig.4a). Due to its excellent elasticity and tensile properties, BCFs can also be made into fabrics that perfectly fit to the surface of the human body, exhibiting outstanding mechanical performance in application.

Table 2: Mechanical property parameters of composite fibers

Sample	Maximum Force(N)	Tensile Strength(Mpa)	Breaking Elongation(%)
PU	0.89	2.34	562.72
PU-TMC$_{0.05}$	0.78	2.05	432.17
PU-TMC$_{0.15}$	0.84	2.19	366.98
PU-TMC$_{0.25}$	0.99	2.59	309.08
PU-TMC$_{0.35}$	1.76	4.59	246.55

Synergistic infrared/visual stealth of BCFs

Visible light invisibility, also known as visual stealth, is primarily achieved by reducing the color difference between the target and the background environment to deceive the human vision. The thermochromic behavior of TMC within the fiber allows BCFs to change color with temperature variations (Fig.5a). Additionally, the photothermal conversion and temperature regulation provided by BCFs can serve as an adjustable heat source for thermochromic responses, enabling adaptive camouflage in the visible light range under changing scenarios. UV-vis-NIR spectroscopy (Fig.5b, c) reveals that, compared to pure PU fiber, BCFs exhibit higher absorption in the near-ultraviolet and visible light range (200-800 nm), with absorption values increasing with the TMC content.

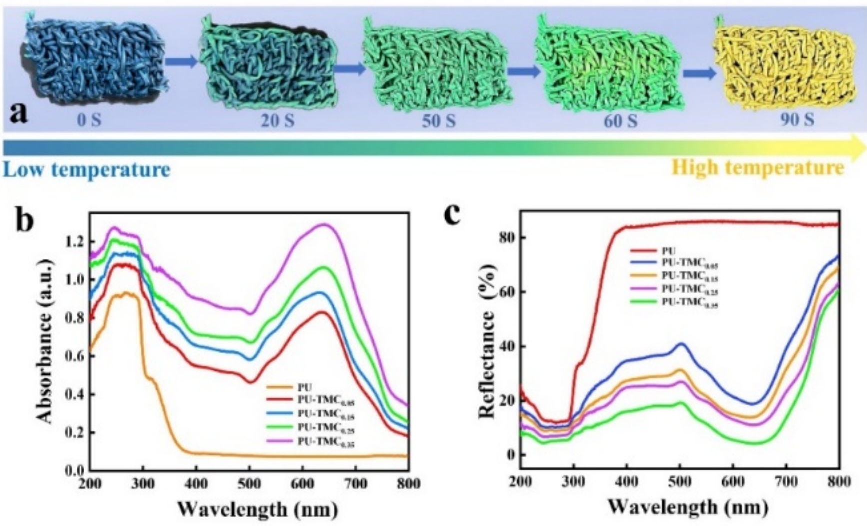

Figure 5: (a) Thermochromic process of fiber samples with temperature changes. (b)UV absorption and (c) reflectance spectra of fibers with different TMC contents

To demonstrate visual stealth performance, the BCFs were woven into fabric and subjected to visual camouflage tests in various backgrounds, simulating the ability to achieve visual invisibility in multiple scenarios including ocean, jungle, and desert environments (Fig.6a-c). As shown in Fig.6d when the samples were placed in simulated seawater, they were challenging to be detected at a glance, which facilitate visual invisibility in deep-sea environments. When the samples were transferred to a jungle setting (Fig.6e), they quickly transformed into green, showing rapid color response characteristics and seamlessly hiding amidst the surrounding vegetation. Under sunlight exposure, the samples spontaneously turned yellow through photothermal conversion, perfectly corresponding to the transition from the cool green jungle to the scorching yellow desert scene (Fig.6f). This demonstrated the rapid solar-driven heating and stable solar thermal conversion characteristics, proving highly beneficial for achieving visual invisibility without restrictions in outdoor and all-weather environments. Importantly, the different PCMs injected into BCFs contribute to temperature regulation in various environments. In the hot desert, the high phase-change temperature of EO can absorb ambient heat and store it, maintaining body temperature in a comfortable range and preventing potential overheating risks. In the cold sea, the low phase-change temperature of HD similarly provides a comfortable microclimate for the body through its heat absorption and release, preventing injuries caused by temperature fluctuations during military operations. In summary, regardless of the outdoor environment, the thermochromic effect and temperature-regulating energy storage capabilities of BCFs drive the fibers to change color dynamically, achieving active thermochromic visual invisibility in dynamic scenarios.

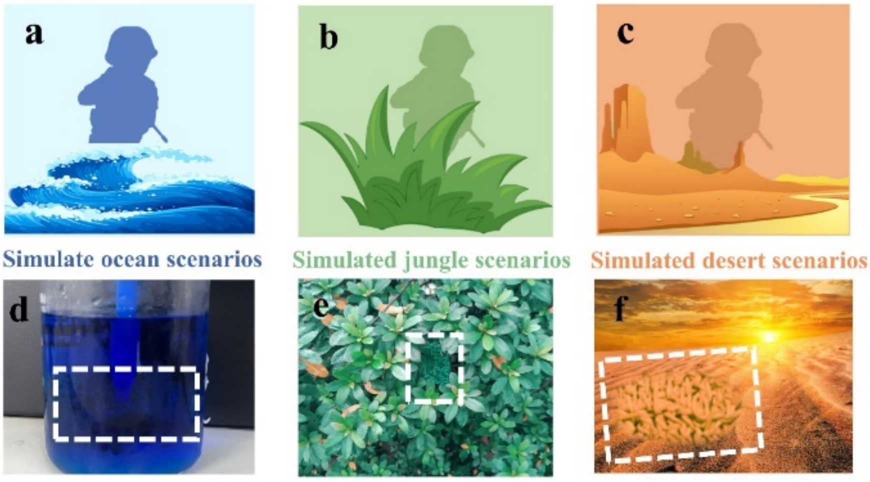

Figure 6: Simulates visual stealth effects: (a, d) ocean (b, e) jungle (c, f) desert

However, with the advancements in technology, sophisticated infrared detection techniques have emerged, capable of identifying discrepancies in infrared radiation among objects and between objects and their background. These detection mechanisms translate the radiation signals into infrared images with discernible color contrasts. Therefore, the integration of techniques for visual stealth and infrared stealth is paramount to prevent the detection of targets. In comparison to visual stealth, infrared stealth involves reducing the infrared radiation intensity of a designated target to align with the background, achieving the effect of concealment. Modulating the temperature difference between the target and the background is a crucial strategy for achieving infrared stealth.

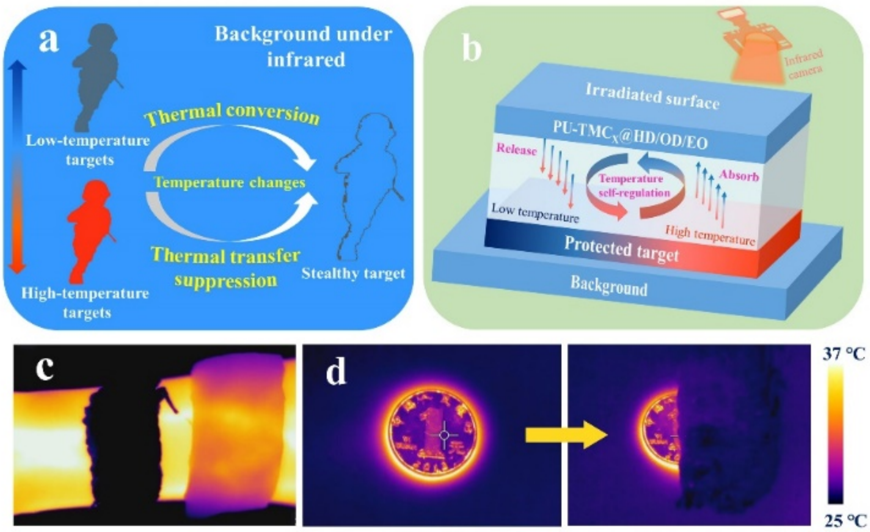

Figure 7: (a) Schematic diagram of IR stealth; (b) IR stealth mechanism of fibers; Under IR camera comparison between samples and normal fabrics (c), and the stealth effect of samples against heated coins (d)

Fig.7a-b elucidates the infrared stealth mechanism of the prepared BCFs. When the temperature of the protected object surpasses the background temperature, the target becomes easily detectable by infrared detectors. However, if covered by BCFs, the heat generated by the protected object can be absorbed by the PCM within the fibers, facilitating temperature regulation and mitigating temperature elevation, thereby reducing the temperature difference with the background. Conversely, when the temperature of the protected object is lower than the background temperature, BCFs can achieve infrared stealth by releasing stored latent heat.

To illustrate the infrared stealth performance of BCFs samples, PU-TMC$_{0.25}$@OD fibers were woven into a BCFs wristband, covering it on the human body, and tested the difference between the prepared samples and regular fabric under an infrared camera. The results showed that the uncovered part on the arm was still clearly detected by the infrared imager (Fig.7c). The temperature of the part covered by regular fabric rapidly increased, displaying a distinct outline. However, the portion covered by the BCFs wristband seamlessly blended with the background, exhibiting infrared radiation similar to its surroundings, making it challenging to detect under the infrared camera. Moreover, to meet the infrared stealth requirements at different temperatures, the phase transition temperature of BCFs samples can be adjusted by controlling the injection of different PCMs. This not only better satisfies the comfort requirements of the human body but also enables effective stealth in multiple temperature zones. To further demonstrate the infrared stealth capability of BCFs samples for protecting objects, a heated coin was placed on the desktop, and half-covered with BCFs samples (Fig.7d). Under the monitoring of the infrared camera, it was evident that one half of the coin's contour was pronounced, while the other half coin completely ‘disappeared’ into the environment, confirming the authentic infrared stealth performance of BCFs samples in practical applications. Clearly, BCFs samples can effectively regulate the surface temperature of protected objects through the absorption and release of heat, thereby reducing the temperature difference between objects and the background, providing an effective thermal management and temperature control strategy for infrared stealth.

In summary, BCFs composites integrate the combined performance of visual stealth and infrared stealth. The adaptive and adjustable appearance of BCFs, coupled with the thermoregulatory effect of the PCM, ensures that the target remains unrecognized in visual environments and covert in infrared imaging. This achieves all-weather, all-round stealth in high and low temperature environments.

Conclusions

In conclusion, this study based on the phase separation principle and utilizing wet spinning, has designed and fabricated a woven composite fiber that integrates both infrared and visual stealth, he prepared composite fibers possess adjustable phase-change temperatures (ranging from 15°C to 38°C), outstanding heat storage capacity (with a sample enthalpy value of up to 147.09 J/g), and remarkable cyclic stability, enduring at least 100 heating-cooling cycles. Furthermore, the mechanical performance of the fibers is exceptional, with a ten-centimeter-length fiber capable of supporting a 200g load without breaking, and easily adaptable for weaving into fabrics or any desired shape. Importantly, the fiber's adaptive color-changing effect perfectively satisfies the requirements for visual stealth in complex scenes within the visible light spectrum. It can be applied in various dynamic scenarios, ranging from marine to jungle to desert environments. Combining outstanding thermal management and temperature control, the fiber concurrently achieves all-weather infrared stealth, overcoming the limitations of conventional stealth technologies. It is evident that this advanced visual/infrared stealth technology holds great application prospects in human concealment, equipment stealth, military target concealment, and beyond. The adaptive stealth design also provides a promising idea for daily thermal management and defense applications, offering new insights for the development of the next generation of stealth technologies.

Declaration of Competing Interest

The authors declare that they have no known competing financial interests or personal relationships that could have appeared to influence the work reported in this paper. On behalf of all authors, the corresponding author states that there is no conflict of interest.

Data availability

Data will be made available on request.

Acknowledgements

The study was supported by Sailing Project from the Science and Technology Commission of Shanghai Municipality (17YF1406600), Chenguang project of Shanghai Municipal Education Commission and Shanghai Education Development Foundation (18CG68), and Shanghai Polytechnic University for funding (EGD23QD03).

References

1. B Wang, G Xu, S Song, Z Ren, D Liu et al. (2022) Flexible, infrared adjustable, thermal radiation control device based on electro-emissive PANI/Ce4+ thin films inspired by chameleon, Chem. Eng. J, 445: 136819.

2. Y Cheng, X Zhang, C Fang, J Chen, Z Wang (2018) Discoloration mechanism, structures and recent applications of thermochromic materials via different methods: A review, J Mater Sci Technol, 34: 2225-34.

3. X Zhai, Z Wu, H Peng (2022) Mini review on Application of Microencapsulated Phase Change Materials with Reversible Chromic Function: Advances and Perspectives, Energy Fuels, 36: 8054-65.

4. J Ahn, T Lim, CS Yeo, T Hong, S-M Jeong et al. (2019) Infrared Invisibility Cloak Based on Polyurethane–Tin Oxide Composite Microtubes, ACS Appl. Mater. Interfaces, 11: 14296-304.

5. W Niu, L Zhang, Y Wang, Z Wang, K Zhao, S Wu et al. (2019) Multicolored Photonic Crystal Carbon Fiber Yarns and Fabrics with Mechanical Robustness for Thermal Management, ACS Appl. Mater. Interfaces, 32261-8.

6. Rq Wang, Yj He, Yy Xiao, Dx Sun, Jh Yang, Xd Qi et al. (2023) Weavable phase change fibers with wide thermal management temperature range, reversible thermochromic and triple shape memory functions towards human thermal management, Eur. Polym, 187: 111890.

7. Y Zhang, G Shen, SS Lam, S Ansar, S-C Jung et al. (2023) A waste textiles-based multilayer composite fabric with superior electromagnetic shielding, infrared stealth and flame retardance for military applications, Chem. Eng J, 471: 144679.

8. T Ma, J Bai, TLi, S Chen, X Ma, J Yin et al. (2021)Light-driven dynamic surface wrinkles for adaptive visible camouflage, Proc. Natl. Acad. Sci. U.S.A. 118.

9. X Hu, M Wu, L Che, J Huang, H Li, Z Liu et al. (2023) Nanoengineering Ultrathin Flexible Pressure Sensor with Superior Sensitivity and Perfect Conformability, Small, 19: 2208015.

10. M Yang, J Pan, L Luo, A Xu, J Huang, Z Xia et al. (2019) CNT/cotton composite yarn for electro-thermochromic textiles, Smart Mater Struct, 28.

11. S. Samanta, S Sarkar, NK Singha (2020) Multifunctional Layer-by-Layer Coating Based on a New Amphiphilic Block Copolymer via RAFT-Mediated Polymerization-Induced Self-Assembly Process, ACS Appl. Mater. Interfaces, 15: 24812-26.

12. C Wang, J Shi, L Zhang, S Fu (2024) Asymmetric Janus Fibers with Bistable Thermochromic and Efficient Solar–Thermal Properties for Personal Thermal Management, Adv. Fiber Mater.

13. J Oh, JW Choi, CT Yavuz, S-Y Chung, JY Park, Y Jung (2017) EEWS 2016: Progress and Perspectives of Energy Science and Technology, ACS Energy Lett, 2: 592-4.

14. B-X Li, Z Luo, W-G Yang, H Sun, Y Ding, Z-Z Yu, D Yang (2023) Adaptive and Adjustable MXene/Reduced Graphene Oxide Hybrid Aerogel Composites Integrated with Phase-Change Material and Thermochromic Coating for Synchronous Visible/Infrared Camouflages, ACS Nano, 17: 6875-85.

15. AW Kandeal, MR Elkadeem, A Kumar Thakur, GB Abdelaziz, R Sathyamurthy et al. (2021) Infrared thermography-based condition monitoring of solar photovoltaic systems: A mini review of recent advances, Solar Energy, 223: 33-43.

16. J Hu, Y Hu, Y Ye, R Shen (2023) Unique applications of carbon materials in infrared stealth: A review, Chem. Eng. J, 452: 139147.

17. Y He, X-W Wu, G Hu, W Ke (2023) A new way to achieve infrared stealth by composite phase change microcapsules, Journal of Energy Storage, 73: 109217.

18. YWu, S Tan, Y Zhao, L Liang, M Zhou, G Ji (2023) Broadband multispectral compatible absorbers for radar, infrared and visible stealth application, Prog. Mater. Sci, 135: 101088.

19. J Gu, W Wang, D Yu (2022) Temperature-control and low emissivity dual-working modular infrared stealth fabric, COLLOID SURFACE A, 653: 129966.

20. J Wang, Z He, Z Du, X Cheng, H Wang, X Du (2023) Highly Stretchable Ti3C2Tx MXene-Integrated Phase Change Films for Solar-Thermal Harvesting and Infrared Stealth, ACS Sustain. Chem. Eng, 11: 13187-97.

21. T Shi, Z Zheng, H Liu, D Wu, X Wang (2023) Flexible and foldable composite films based on polyimide/phosphorene hybrid aerogel and phase change material for infrared stealth and thermal camouflage, Compos Sci Technol, 217: 109127.

22. Z Han, Y Shen, C Li, R Chen, JLi, S Guo (2023) Enhancement of infrared stealth performance of ultra-high molecular weight polyethylene-based composites through the multilayer structural construction, Compos Sci Technol, 241: 110150.

23. D.G. Prajapati, B. Kandasubramanian, A Review on Polymeric-Based Phase Change Material for Thermo-Regulating Fabric Application, Polym Rev (2020) 389-419.

24. Y Chen, Q Ma, L Chen, X Wang, X Zhao, N Bing et al. (2023) Enhanced light-to-thermal conversion performance of self--assembly carbon nanotube/graphene-interconnected phase change materials for thermal-electric device, J Energy Storage, 72: 108387.

25. Q Ma, X Wang, Y Chen, L Chen, L Zhang, X Zhao et al. (2023) Poly(vinyl alcohol)-Based Nanofibers with Improved Thermal Conductivity and Efficient Photothermal Response for Wearable Thermal Management, ACS Appl. Nano Mater, 6: 14733-44.

26. J Xu, X Zhang, L Zou (2022) A review: Progress and perspectives of research on the functionalities of phase change materials, J Energy Storage, 54: 105341.

27. C Wen, B Zhao, Y Liu, C Xu, Y Wu et al. (2023) Che, Flexible MXene-Based Composite Films for Multi-Spectra Defense in Radar, Infrared and Visible Light Bands, Adv. Funct. Mater, 33.

28. YC Zhou, J Yang, L Bai, R-Y Bao, M-B Yang, W Yang (2023) Flexible phase change hydrogels for mid/low-temperature infrared stealth, Chem. Eng. J, 137463.

29. Y Zhao, G Ji (2022) Multi-spectrum bands compatibility: New trends in stealth materials research, Sci. China Mater, 65: 2936-2941.

30. J Chen, S Zhang, Y Wei, J Yi, W Pang et al. (2023) Flexible human-applicable infrared camouflage materials with temperature and emissivity tunability, Compos Sci Technol, 233: 109920.